

**Antibacterial mechanism of chitosan-gentamicin and its effect on the intestinal flora
of *Litopenaeus vannamei* infected with *Vibrio parahaemolyticus***

Lefan Li¹, Fengyan Liang^{1,2,3*}, Chengpeng Li¹ Tingting Hou¹ and Dong-an Xu¹

¹ School of Chemistry and Environment Science, Guangdong Ocean University, Zhanjiang 524088, China
FLL@gdou.edu.cn (L.L.); lcp0802@126.com (C.L.); ht415@126.com (T.H.)

² Life Science & Technology School, LingNan Normal University, Zhanjiang 524048, China

³ Mangrove Institute, LingNan Normal University, Zhanjiang 524048, China

*Correspondence: yaner204126@163.com; Tel.: +86 18319379880

1.Tables

Table S1. Inhibition rate and IC₅₀ of *V. parahaemolyticus* dealt with CS, GT and CS-GT ($\bar{x} \pm SD$, n=3)

Sample	Inhibition rate(%, 20 μ g/mL)	IC ₅₀ (μ g/mL)
CS	12.36±4.10 ^c	125.62±4.35 ^a
CS-GT	77.72±5.31 ^b	18.72±3.17 ^b
GT	97.38±3.20 ^a	7.89±5.08 ^c

Note: a,b,c indicate statistically significant variations in the same column, $p < 0.01$.

Table S2. The increase multiple of OD₂₆₀ and K⁺, increase multiple of conductivity dealt with CS, GT and CS-GT at 12 h ($\bar{x} \pm SD$, n=3)

Sample	OD ₂₆₀ increase multiple	K ⁺ increase multiple	Conductivity rate (%)	increase
CK	/	/	/	
CS	5.80±0.21 ^c	24.41±4.30 ^b	8.53±0.05 ^b	
GT	11.56±0.33 ^a	43.70±4.23 ^a	17.71±0.05 ^a	
CS-GT	8.62±0.22 ^b	39.52±5.01 ^a	15.35±0.04 ^a	

Note: “/” means no data provided; a,b,c indicate statistically significant variations in the same column, $p < 0.05$.

Table S3. Composition and relative abundance of gut microbial communities at phylum level ($\bar{x} \pm SD$, n=3)

Group	Tenericutes (%)	Proteobacteri a (%)	Firmicutes (%)	Bacteroidete s (%)
CK	4.41±0.12 ^d	34.57±1.53 ^b	16.33±3.46 ^b	34.95±1.26 ^a
Only-infected group	3.32±0.18 ^d	59.99±1.65 ^a	21.41±6.96 ^b	13.65±4.72 ^c
CS-GT-10	18.68±5.15 ^c	54.65±1.02 ^a	5.78±0.32 ^c	5.86±0.64 ^d
CS-GT-50	58.25±0.27 ^b	4.03±0.07 ^c	11.12±7.72 ^b	16.01±5.31 ^c
CS-GT-100	79.05±1.22 ^a	7.95±0.35 ^c	3.76±0.35 ^c	6.78±0.59 ^d
GT-10	1.68±0.23 ^d	5.41±0.35 ^c	37.37±1.09 ^a	36.52±1.72 ^a
CS-250	23.75±7.31 ^c	34.54±1.23 ^b	34.87±4.41 ^a	25.26±2.34 ^b

Note: a,b,c indicate statistically significant variations in the same column, $p < 0.05$

Table S4. Relative intensities of the fitted C1s peak of CS, OCS, GT, P-CS-GT and CS-GT.

Sample	Position (eV)	Relative intensity (%)	Possible element state
CS	285.2	50.73%	C-C/C-H
	286.7	30.16%	C-N
	288.3	13.17%	C-O

	289.2	5.64%	C=O
OCS	285.0	56.27%	C-C/C-H
	286.7	20.53%	C-N
	288.4	10.56%	C-O
	289.2	12.64%	C=O
GT	285.2	50.33%	C-C/C-H
	286.7	36.73%	C-N
	288.4	12.94%	C-O
P-CS-GT	285.0	38.10%	C-C/C-H
	286.7	27.58%	C-N
	287.5	19.16%	C=N
	288.4	10.74%	C-O
	289.3	4.42%	C=O
CS-GT	285.7	42.42%	C-C/C-H
	286.7	29.48%	C-N
	287.5	10.08%	C=N
	288.5	12.24%	C-O
	289.5	5.77%	C=O

2.Figures

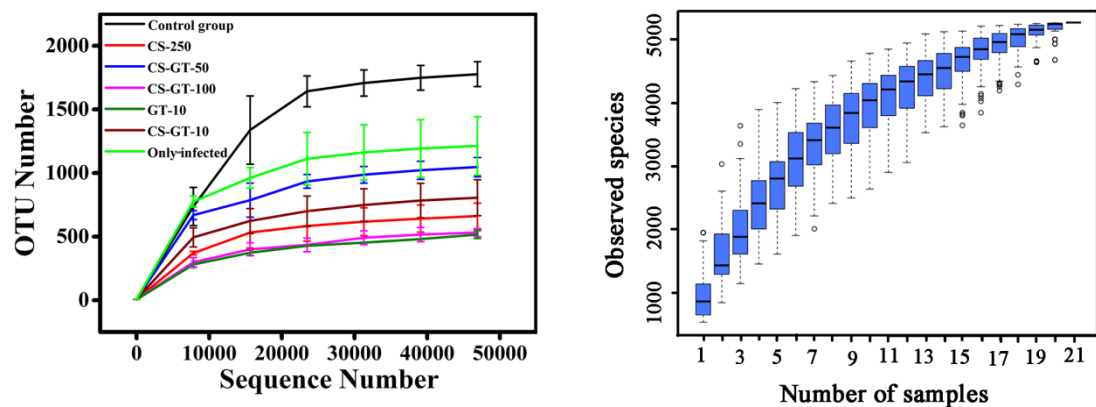


Figure S1. Rarefaction curves and species accumulation box diagram of intestine samples ($\bar{x} \pm SD$, n = 3)

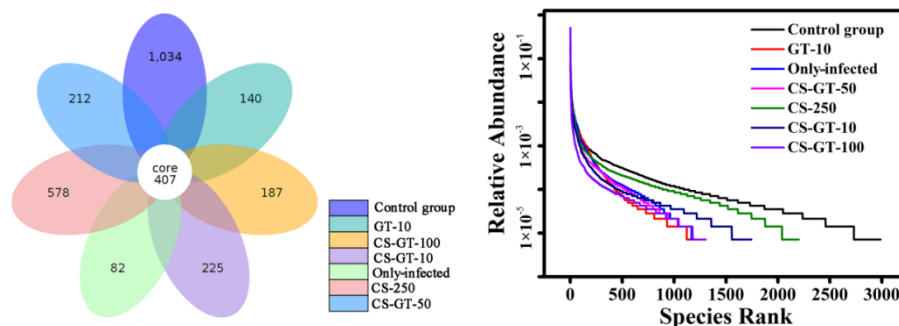


Figure S2. Venn diagram of operational taxonomic unit (OTU) numbers and rank abundance curve ($\bar{x} \pm SD$, n=3)

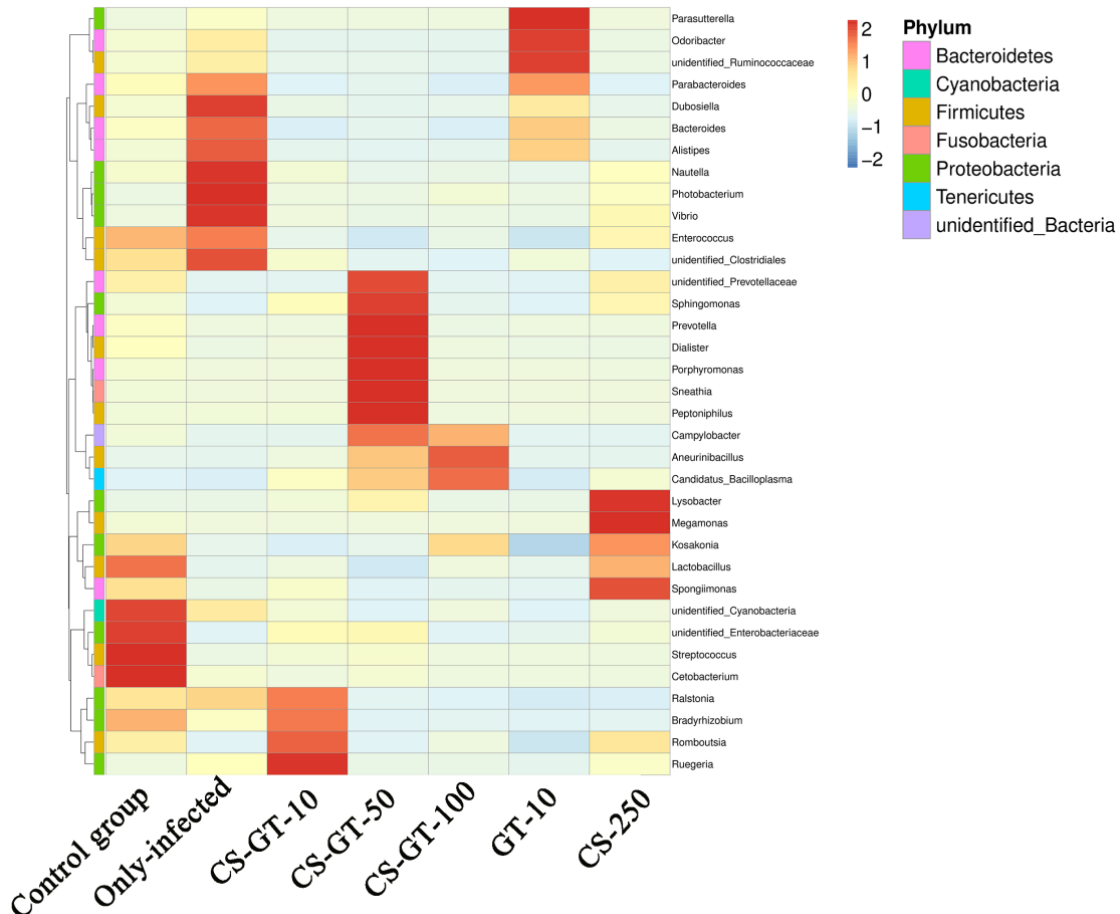


Figure S3. Heatmap of the species abundance clustering in the top 35 at the genus level ($\bar{x} \pm SD$, n=3)

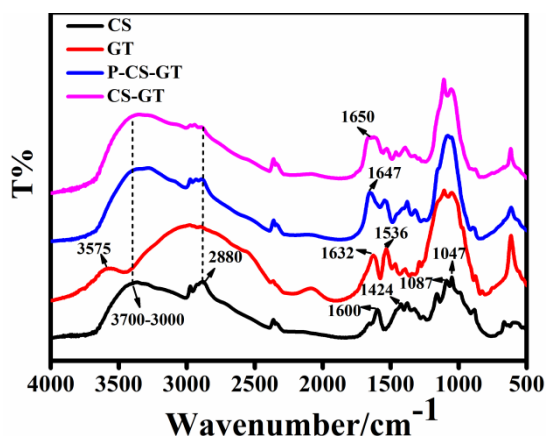


Figure S4. The FTIR spectrum of CS, GT, P-CS-GT (C=N) and CS-GT (C-N).

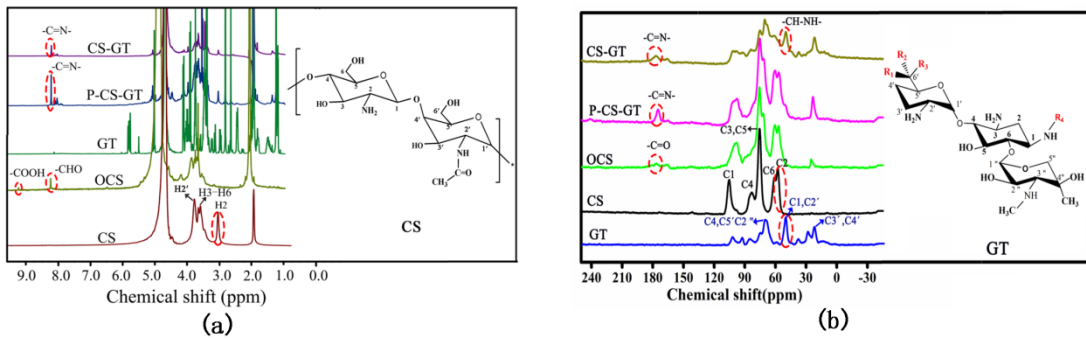


Figure S5. The ¹H-NMR (a) and solid-state ¹³C-NMR spectrum of CS, OCS, GT, P-CS-GT and CS-GT.

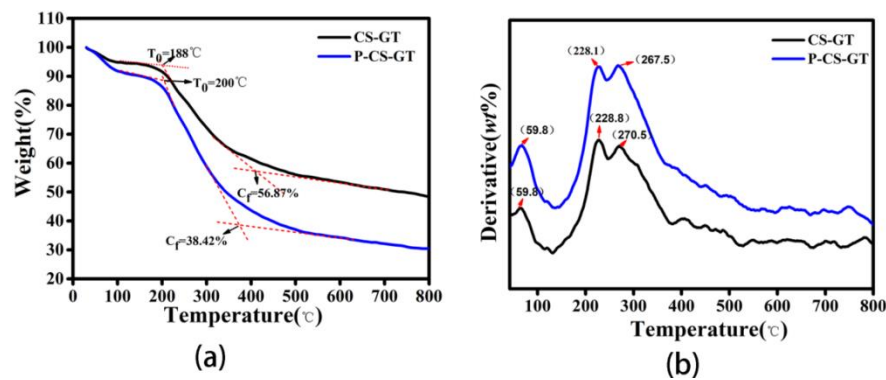


Figure S6. The TG curves (a) and DTG curves (b) of P-CS-GT and CS-GT.